Cleveland State University
EngagedScholarship@CSU

Mechanical Engineering Faculty Publications | Mechanical Engineering Department

9-2009

An Elaborate Data Set Characterizing the Mechanical Response of the Foot

Ahmet Erdemir
Cleveland Clinic, erdemira@ccf.org

Pavana A. Sirimamilla
Cleveland Clinic

Jason P. Halloran
Cleveland Clinic

Antonie J. van den Bogert
Cleveland State University, a.vandenbogert@csuohio.edu

Follow this and additional works at: https://engagedscholarship.csuohio.edu/enme_facpub

 Part of the Biomechanical Engineering Commons

How does access to this work benefit you? Let us know!

Original Citation

Erdemir, A., Sirimamilla, P. A., Halloran, J. P., and van den Boger, A. J., 2009, "An Elaborate Data Set Characterizing the Mechanical Response of the Foot," Journal of Biomechanical Engineering, 131(9) pp. 094502-094502.

This Article is brought to you for free and open access by the Mechanical Engineering Department at EngagedScholarship@CSU. It has been accepted for inclusion in Mechanical Engineering Faculty Publications by an authorized administrator of EngagedScholarship@CSU. For more information, please contact library.es@csuohio.edu.

An Elaborate Data Set Characterizing the Mechanical Response of the Foot

Ahmet Erdemir[1]
Department of Biomedical Engineering,
Cleveland Clinic,
Cleveland, OH 44195;
Computational Biomodeling Core,
Lerner Research Institute,
Cleveland Clinic,
Cleveland, OH 44195
e-mail: erdemira@ccf.org

Pavana A. Sirimamilla
Department of Biomedical Engineering,
Cleveland Clinic,
Cleveland, OH 44195;
Department of Mechanical and Aerospace Engineering,
Case Western Reserve University,
Cleveland, OH 44106

Jason P. Halloran

Antonie J. van den Bogert

Department of Biomedical Engineering,
Cleveland Clinic,
Cleveland, OH 44195

Mechanical properties of the foot are responsible for its normal function and play a role in various clinical problems. Specifically, we are interested in quantification of foot mechanical properties to assist the development of computational models for movement analysis and detailed simulations of tissue deformation. Current available data are specific to a foot region and the loading scenarios are limited to a single direction. A data set that incorporates regional response, to quantify individual function of foot components, as well as the overall response, to illustrate their combined operation, does not exist. Furthermore, the combined three-dimensional loading scenarios while measuring the complete three-dimensional deformation response are lacking. When combined with an anatomical image data set, development of anatomically realistic and mechanically validated models becomes possible. Therefore, the goal of this study was to record and disseminate the mechanical response of a foot specimen, supported by imaging data. Robotic testing was conducted at the rear foot, forefoot, metatarsal heads, and the foot as a whole. Complex foot deformations were induced by single mode loading, e.g., compression, and combined loading, e.g., compression and shear. Small and large indenters were used for heel and metatarsal head loading, an elevated platform was utilized to isolate the rear foot and forefoot, and a full platform compressed the whole foot. Three-dimensional tool movements and reaction loads were recorded simultaneously. Computed tomography scans of the same specimen were collected for anatomical reconstruction a priori. The three-dimensional mechanical response of the specimen was nonlinear and viscoelastic. A low stiffness region was observed starting with contact between the tool and foot regions, increasing with loading. Loading and unloading responses portrayed hysteresis. Loading range ensured capturing the toe and linear regions of the load deformation curves for the dominant loading direction, with the rates approximating those of walking. A large data set was successfully obtained to characterize the overall and the regional mechanical responses of an intact foot specimen under single and combined loads. Medical imaging complemented the mechanical testing data to establish the potential relationship between the anatomical architecture and mechanical responses and to further develop foot models that are mechanically realistic and anatomically consistent. This combined data set has been documented and disseminated in the public domain to promote future development in foot biomechanics.

Keywords: foot biomechanics, heel, metatarsal heads, tarsometatarsal joint, arch properties, plantar tissue deformation

1 Introduction

The foot is the interface between the body and ground or footwear during locomotion, and undergoes large loads and deformations. Knowledge of its mechanical response potentially elucidates the causative factors of mechanical dysfunction as a result of abnormal tissue structures and mobility of foot joints. Description of foot mechanics also forms the basis to establish its representation in computational analysis that focuses on the investigation of human movement [1]. In a similar manner, predictive exploration of foot disorders [2] and therapeutic or performance related interventions, applied to the foot or its components [3], is possible.

The passive load-deformation behavior of the foot is dictated by plantar tissue properties and the properties of foot joints. Numerous studies have been conducted to investigate the overall stiffness of the foot and the arch [4]. Structural testing studies also quantified stiffness properties of various foot joints [5]. Testing of intact regions of the foot, e.g., heel [6,7], identified regional response due to the underlying plantar tissue. Mechanical loading of tissue samples extracted from the heel [8] or the forefoot [9] aided in reconstruction of material models for plantar tissue [9,10]. The majority of previous studies tested only the region of interest, it being the whole foot [4,11], the heel [12], or the forefoot [13], in isolation. Characterization of a foot, including its overall response and the response of its key individual components, is lacking. Loading modes were also limited to a single direction, commonly compressing the tissue [8,9] or the foot [7,11]. While this approach establishes foot response in a dominant loading case of daily activities, three-dimensional representation of foot stiffness and the material properties of its tissues can be critical for predictive purposes [14,15].

Association of the anatomical details of the foot to mechanical data is also important from a modeling perspective. The value of such an association has been recognized [13], yet, a comprehensive testing scheme has not been employed. Anthropometric data, relative joint positions, and regional description of tissue stiffness, for example, are critical in building realistic and validated models of the foot for gait analysis [16] and musculoskeletal simulations [17]. Tissue level geometric detail when supported by mechanical response obtained using the same foot is indispensable in realizing accurate models for finite element analysis [18–21]. It is common that in many foot models [2,18–20], the source of structural and/or material properties does not match that of the anatomical reconstruction.

Our goal was to quantify the detailed mechanical response of a foot, supported by medical imaging for anatomical reconstruction. In the spirit of similar studies conducted for musculoskeletal simulations [22–24], this data set is also targeted to become a

[1]Corresponding author.

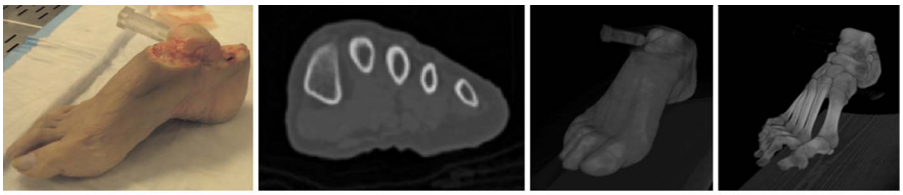

(*a*) (*b*) (*c*) (*d*)

Fig. 1 (a) The foot specimen used for mechanical testing and anatomical imaging. (b) A cross-sectional image at the level of mid metatarsals as obtained from computed tomography. ((c) and (d)) Volumetric reconstruction of computed tomography scans for the foot boundary and the bones.

reference while building foot models representative of its mechanical response. Portrayal of intact response was aimed rather than testing of regions in full isolation, in order to recognize the potential to establish contribution of individual regions to the foot's overall response. Rear foot testing was aimed to record plantar tissue response whereas forefoot testing was targeted at measuring overall deformation characteristics of the arch. Loading of metatarsal head regions provided mechanical response of the individual rays of the foot. Whole foot deformations quantified foot mechanics as a complete entity. The final objective of this work was to disseminate the data set in full detail, with the intent to expedite prospective studies in foot biomechanics.

2 Methods

The specimen was a right foot from a male Caucasian donor (Fig. 1(*a*)). At the time of death, the age of the donor was 58 years; bodyweight and height were 79.4 kg and 1.73 m, respectively. Foot length was 0.24 m, measured from the posterior aspect of the heel to the tip of the second toe. Foot width was 0.09 m and its height was 0.08 m. The width of the foot corresponded to the distance between the medial aspect of the first metatarsal head and the lateral aspect of the fifth metatarsal head. Foot height was measured when the foot was resting on its own weight, from resting surface to the superior aspect of the navicular.

Prior to mechanical testing, computed tomography scans were obtained while the foot was resting on its own weight on a flat surface (Fig. 1(*b*)). Before imaging, a registration phantom was screwed in the talus. The phantom was made out of Plexiglas and filled with water with the intent to register anatomical images with coordinate systems of mechanical testing. Axial images (a total of 288) were recorded using a Siemens computed tomography system (SOMATOM Sensation 64, Siemens Medical Solutions USA, Inc., Malven, PA) at a resolution of 512×512 pixels. The pixel size was 0.365234 mm and the spacing between the images was 1 mm. In this study, the three-dimensional visualization of computed tomography scans (Figs. 1(*c*) and 1(*d*)) were accomplished with VolSuite.[2]

Mechanical testing was conducted on a six degree of freedom parallel robotic system (Rotopod R2000, Parallel Robotic Systems Corp., Hampton, NH) controlled with stepper motors (Fig. 2(*a*)). The robot base contained a stationary coordinate system (R) and the platform of the robot had a moving coordinate system (P) relative to the base (Fig. 2(*a*)). At a zeroed state, approximately at the midpoint of the range of the robot, these coordinate systems were coincident and aligned at the center of the platform. The z-axis pointed upwards, and the x- and y-axes defined the plane of the platform. The range of motion of the robot was ± 0.1 m in the x- and y-axes with a rotation capacity of ± 10 deg. In the z-axis the range was ± 0.1 m and ± 720 deg. The factory specified movement accuracy of the robot was 50 μm, with a repeatability of 25 μm [25]. The desired robot trajectory (position and orientation) was provided at a sample rate of 50 Hz and was recorded.

The reaction forces and moments, generated on the specimen during the experiments, were recorded using a spatial load cell (Theta, ATI Industries Corp., Apex, NC). The load cell was attached to the main frame of the experimental setup, with the origin of its coordinate system (L) at the transducer center and orientation was as illustrated in Fig. 2 based on the description of the supplier. The load cell had 0.5 N (1.1 N in the z-direction) and 0.07 N m force and moment measurement resolutions, respectively. During experimentation, load cell data were recorded at a sampling rate of 1000 Hz.

For experiments, the foot was first prepared by removing excess tissue around the talus (Fig. 1(*a*)). The talus and calcaneus were fixed relative to each other by passing screws through both. In following, the superior part of the rear foot was firmly attached to an aluminum fixture, using denture base and repair resin (NATURE-CRYL® POUR, GC America, Inc., Alsip, IL). An aluminum support rod attached the fixture to a steel load cell interface component (Fig. 2(*a*)).

Various tools were placed on the robot platform to test desired regions of the foot, or the whole foot (Fig. 2(*a*)). For indentation, large and small steel spheres were used (0.0254 m and 0.0127 m in diameter, respectively). Rear foot and forefoot isolations were accomplished with an elevated platform with the dimensions of $0.086 \times 0.051 \times 0.151$ m^3 (width $\times$ height $\times$ length). A full platform effectively covered the surface of the robot platform to facilitate whole foot testing. For the indenters, y-axis of the tool coordinate system (T) was parallel to the z-axis of the platform coordinate system and the origin was located at the tip of the indenter. For the elevated platform, the origin of the tool coordinate system was at the corner of the tool, y-axis in parallel with the z-axis of the platform coordinate system, x-axis along the width, and z-axis along the length of the tool. For the whole platform, the origin of the tool coordinate system was an arbitrary point and the y-axis was in parallel with the z-axis of the platform coordinate system.

A three-dimensional digitizer (Microscribe G2L, Immersion Corp, San Jose, CA; 130 μm resolution and 430 μm accuracy) was used to establish transformation matrices obtained from the relative position and orientation of stationary coordinate systems [25,26]. For this purpose, points were sampled on the robot, platform, load cell, and tools in the digitizer coordinate system (M) [25,26]. As the platform position and orientation were prescribed by the robot, utilization of these transformation matrices allowed tool position and orientation as well as load cell measurements to be represented in any desired coordinate system. The digitizer was also utilized to record points on the anterior, superior, and lateral surfaces of the registration phantom for alignment with the computed tomography coordinate system. In addition, four anatomical landmarks were collected on the foot: posterior aspect of the heel approximately at the calcaneal tuberosity, tip of the second toe, medial aspect of the first metatarsal head, and lateral aspect of the

[2]http://www.osc.edu/archive/VolSuite/.

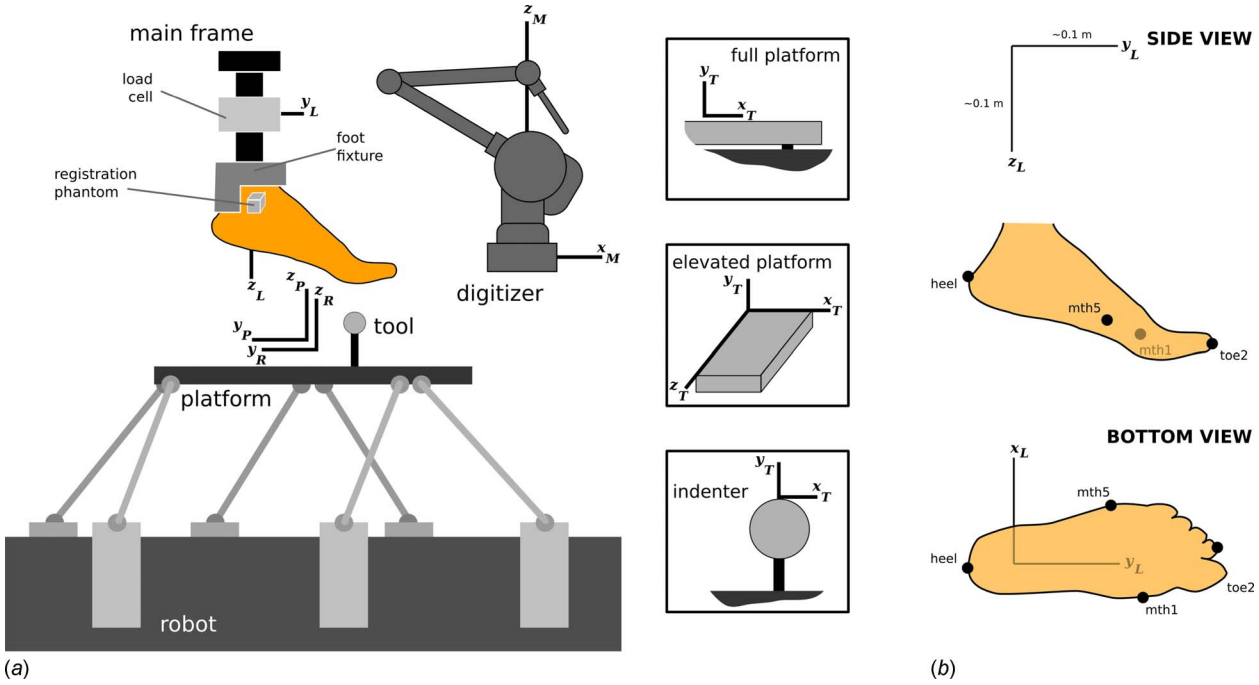

Fig. 2 (a) Experimental setup illustrating assembly of all testing components and the foot, with their associated right-handed coordinate systems (R: robot; P: platform; T: tool; L: load cell; M: Microscribe three-dimensional digitizer (Immersion Corp., San Jose, CA)). (b) Anatomical landmarks digitized on the foot in relation to load cell coordinate system. This coordinate system was used to report foot loading and tool movement data.

Table 1 Mechanical tests conducted on the foot specimen. Mode denotes dominant loading direction induced by tool movement. Range (min/max) corresponds to the reaction loads measured at the origin of the load cell coordinate system. Whole foot loading data sets involve multiple orientations of the tool relative to the foot. All data were represented in the load cell coordinate system.

			Loading Ranges					
Region	Tool	Mode	F_x (N)	F_y (N)	F_z (N)	M_x (N m)	M_y (N m)	M_z (N m)
Forefoot	EP	CS	−24.8/2.3	−7.7/33.0	−3.2/147.3	−0.09/20.49	−3.42/0.01	−0.21/3.30
Forefoot	EP	CS	−29.9/1.4	−11.3/48.0	−2.7/158.7	−0.25/19.81	−4.49/−0.03	−0.16/3.83
Forefoot	EP	CS	−67.2/1.8	−2.8/99.4	−3.5/347.3	−0.11/41.03	−9.25/−0.03	−0.16/8.62
Forefoot	EP	C	−29.8/1.8	−3.2/23.8	−1.9/168.4	−0.15/19.38	−4.32/−0.00	−0.21/4.08
Forefoot	EP	C	−79.6/1.3	−2.8/95.6	−2.7/396.3	−0.10/35.59	−11.38/−0.04	−0.14/10.14
Metatarsal Head 1	SI	C	−1.3/1.9	−11.5/0.6	−3.1/45.1	−0.11/9.14	−0.78/−0.01	−0.31/0.25
Metatarsal Head 2	SI	C	−0.7/3.3	−2.3/2.3	−2.7/42.6	−0.06/5.67	−0.46/0.58	−0.23/0.20
Metatarsal Head 3	SI	C	−2.0/2.5	−6.2/1.4	−4.0/40.7	−0.08/7.01	−0.42/0.78	−0.09/0.24
Metatarsal Head 4	SI	C	−4.1/1.7	−2.6/5.9	−4.1/42.8	−0.15/3.48	−0.52/0.10	−0.14/0.42
Metatarsal Head 5	SI	C	−10.0/1.4	−2.0/5.3	−3.3/34.9	−0.09/2.10	−1.23/0.09	−0.07/0.97
Rear foot	EP	CS	−4.1/1.2	−28.7/4.3	−3.4/87.4	−2.00/6.89	−1.11/0.07	−0.24/0.15
Rear foot	EP	CS	−10.5/0.8	−69.8/3.0	−1.5/273.8	−4.13/15.46	−3.20/0.04	−0.40/0.06
Rear foot	EP	C	−2.7/1.2	−11.3/0.8	−1.4/81.6	−0.12/1.87	−0.95/0.06	−0.13/0.18
Rear foot	EP	C	−8.6/1.5	−31.0/0.9	−1.3/272.1	−0.10/4.73	−3.00/0.02	−0.35/0.22
Rear foot	EP	C	−16.0/2.4	−54.3/0.6	−0.4/514.0	−0.06/7.58	−5.69/−0.02	−0.65/0.22
Rear foot	LI	CS	−10.6/1.2	−24.2/8.4	−3.9/58.4	−2.67/5.85	−2.75/0.15	−0.20/0.16
Rear foot	LI	CS	−66.7/1.3	−93.7/17.3	−2.1/320.2	−7.29/21.11	−16.25/0.03	−0.55/0.19
Rear foot	LI	C	−5.5/1.2	−7.0/0.4	−3.9/31.7	−0.11/1.31	−1.37/0.08	−0.10/0.19
Rear foot	LI	C	−21.8/0.8	−24.9/0.8	−2.6/110.5	−0.09/4.73	−5.31/0.11	−0.19/0.21
Rear foot	LI	C	−21.8/2.9	−25.3/1.5	−2.2/112.1	−0.09/4.88	−5.37/0.06	−0.18/0.21
Rear foot	LI	C	−36.6/0.8	−42.6/0.8	−3.5/191.2	−0.09/7.87	−9.03/0.08	−0.36/0.19
Whole foot	FP	C	−8.1/1.7	−1.9/33.4	−2.6/549.4	−1.29/12.59	−1.86/0.09	−0.14/1.29
Whole foot	FP	C	−35.4/1.3	−3.3/32.7	−2.0/687.4	−0.99/16.42	−9.33/0.06	−0.11/2.50
Whole foot	FP	C	−1.0/30.5	−31.8/16.6	−0.3/783.3	−0.09/22.95	−0.24/6.04	−0.12/0.62
Whole foot	FP	C	−35.0/1.9	−2.2/95.2	−1.9/668.2	−0.31/12.60	−8.05/0.04	−0.17/4.22
Whole foot	FP	C	−7.1/2.5	−2.0/63.8	−2.2/583.3	−0.14/16.88	−1.24/0.02	−0.13/1.91
Whole foot	FP	C	−60.1/0.9	−2.1/78.9	−1.8/615.0	−0.21/13.85	−13.86/0.02	−0.16/5.45
Whole foot	FP	C	−124.5/1.3	−1.5/419.1	−0.8/765.7	−14.73/6.47	−25.24/−0.00	−0.18/13.65

EP: elevated platform; SI: small indenter; LI: large indenter; FP: full platform; C: compression; CS: compression + shear.

fifth metatarsal head (Fig. 2(*b*)). These points establish an anatomically relevant coordinate system and also aid in registration between imaging and mechanical testing data.

Mechanical testing protocols, in particular, control of robot trajectory and data collection, were implemented through a custom software written in LABVIEW (National Instruments Corp., Austin, TX) [26]. Mechanical testing was conducted on the rear foot, forefoot, metatarsal heads, and the whole foot, using the aforementioned tools (Table 1). Two types of loading scenarios were commonly applied. In a compression dominant test, the tool was pressed against the region of interest along a superior direction. A combined loading test compressed the region with the tool up to a specified point, followed by shear displacement at that level to induce multimodal loading. The target position of the tool was identified for a desired force accumulation by moving the robot at a slow loading rate (0.01 m/s). Once determined, the tool was moved to that position at a speed of 0.04 m/s to approximate lifelike loading rates [27,12]. Ten cycles were employed, during which the tool was retracted to unload the foot region. This study reports sample data sets extracted for the tenth cycle and presented in the load cell coordinate system (Fig. 2(*b*)). All load cell data are raw, while the tool position and orientation data were resampled at 1000 Hz using MATLAB (Mathworks, Inc., Natick, MA).

3 Results

Computed tomography provided a clear differentiation of the soft tissue boundary of the foot (Fig. 1(*b*)) and its bones (Fig. 1(*d*)). The rear foot and forefoot were tested under single and combined loading schemes using multiple tools, with forces sometimes exceeding half the bodyweight (Table 1). Metatarsal head testing focused on indentation, whereas whole foot testing included compression of up to one bodyweight (Table 1). The time history of the loading scenarios illustrated the evolution of reaction forces and moments as the tool was positioned to interact with the foot (Fig. 3). In combined load cases, a coupled loading response was apparent as illustrated for rear foot compression and shear (Figs. 3(*a*) and 4). Even in a single loading case, when the tool was moved in a dominant direction, coupling was observed, potentially due to coordinate system selection and the relative alignment of the foot and load transducer (Fig. 3(*b*)). For forefoot regions and the metatarsal heads, the response was a function of tissue deformation and arch stiffness. It is likely that this response was dictated by the tissue at low forces and the tarsometatarsal joint properties at higher forces (Fig. 3(*b*)). In all tests, the mechanical response was nonlinear and exhibited hysteresis (Fig. 4).

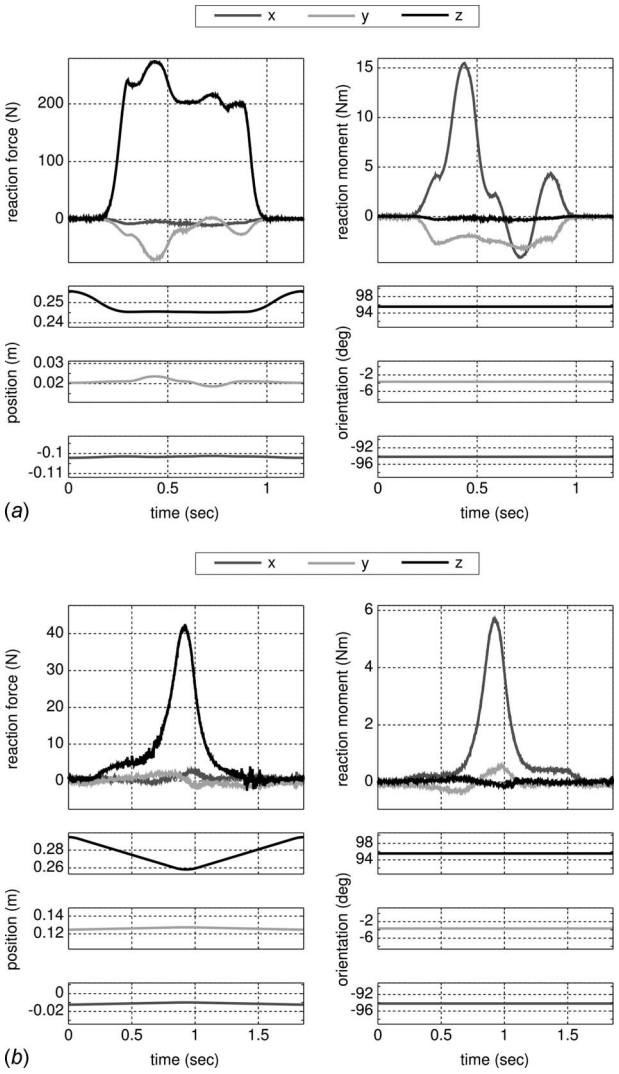

Fig. 3 Time history of foot loading and tool movements presented in the load cell coordinate system. Loading corresponds to reaction forces and moments recorded at the origin of the load cell coordinate system. Kinematics describes the position and orientation of the tool coordinate system relative to the load cell coordinate system. (a) Rear foot compression and shear using the elevated platform. (b) Indentation of the second metatarsal head region using a small indenter (12.7 mm diameter).

4 Discussion

The mechanical response of a cadaver foot was documented in detail, which includes the global and regional tissue responses for specific regions of the foot. Deformation was induced through single and combined loading modes, using multiple tools, at rates representative of daily locomotion. Regional response was qualitatively similar to those obtained previously, e.g., for the heel [6]. To expedite foot biomechanics research, the data are provided in full, freely accessible through the means described in the Appendix.

An apparent limitation of the study was the constriction of the data to a single specimen. The extent of the viscoelastic response was limited to the loading and unloading cases as we did not conduct standardized tests to adequately characterize such behavior [28]. Yet, the loading rates and scenarios utilized were representative of daily locomotion [27]. Apart from these limitations, the range of mechanical loading and the regions tested for this single foot were extensive. Complementing the mechanical response with anatomical imaging also opens many future possibilities. A certain limitation in previous computational studies [29–31], even those conducted on the foot [32], was the lack of specimen specific mechanical data, from which model parameters, e.g., material coefficients, can be estimated, and by which simulation results are validated. This study overcomes these limitations by providing data from both of these domains to build anatomically realistic and mechanically consistent models of the foot.

In an attempt to illustrate tool path relative to the computed tomography scan of the foot, a registration between mechanical testing data and the image set was conducted using a rigid body transformation [33]. The process utilized anatomical landmarks of the foot collected during testing and also extracted from the image sets using VolSuite. In the following, different tool trajectories were overlayed on a volumetric reconstruction of the computed tomography data using VolSuite (Fig. 5). While this process can employ the registration phantom, using foot landmarks accommodates potential differences between relative forefoot and rear foot position in imaging and mechanical testings. With the advent of inverse analysis techniques utilizing anatomically detailed models

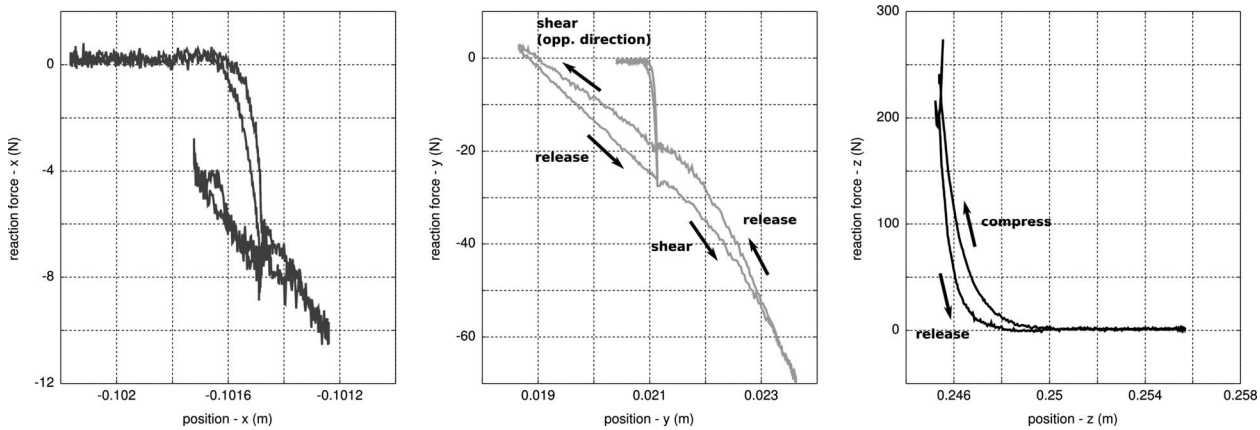

Fig. 4 Reaction forces against tool position. This representation of data from rear foot compression and shear, as applied by the elevated platform, points out the nonlinear nature of foot deformation characteristics. Hysteresis is noticeable as illustrated by the differences in loading and unloading patterns. Tool movement in the shear direction was applied at a fixed tool position in the compression direction. Reaction moments and tool orientation were not shown since tool orientation was kept constant during the test. All data were represented in the load cell coordinate system.

obtained from such image sets [34], the loading data can be used to estimate plantar tissue properties and deformation characteristics of the joints at the arch of the foot.

Our future work will benefit from this data set to establish comprehensively validated, anatomically detailed, and mechanically representative models of the foot using finite element analysis. The present work was limited to the passive properties of the foot. We envision that muscle function can be represented by additional line elements, in which force is generated by mathematical models of muscle contraction, e.g., see Ref. [1]. The combination of both techniques will allow musculoskeletal movement simulations and for the investigation of foot tissue and joint deformations [35]. Dissemination of the whole data set will hopefully facilitate investigators in foot biomechanics to take similar paths to accommodate their research needs.

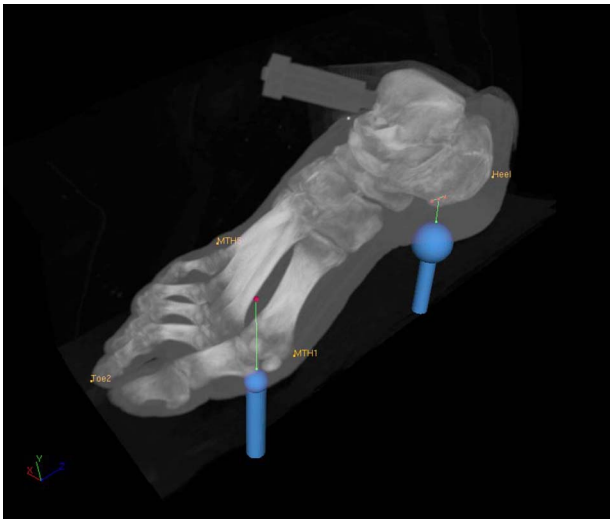

Fig. 5 Tool trajectories overlayed on volumetric reconstruction of computed tomography data. Paths of the large indenter (25.4 mm diameter) during rear foot compression and shear and the small indenter (12.7 mm diameter) during compression of the first metatarsal head region are illustrated. Registration between mechanical testing data and computed tomography scans was accomplished using anatomical landmarks measured during robotic testing and extracted from images as well.

Acknowledgment

The authors are thankful for the efforts of Joshua Polster, MD, of Diagnostic Radiology, Cleveland Clinic, who made computed tomography scanning possible; and Robb Colbrunn, MS, of Musculoskeletal Robotics and Mechanical Testing Core in the Department of Biomedical Engineering, Cleveland Clinic, who provided his expertise on robotic testing. The study was funded by the NIBIB, NIH Grant No. 5R01EB006735, in collaboration with Simbios, NIH Center for Biomedical Computation at Stanford University. The testing facility was partially supported by the NIAMS, NIH Core Center Grant No. 1P30AR050953.

Appendix

Full data set, including mechanical testing and computed tomography, is freely accessible in the "Downloads" section of the project website.[3] Alternatively, interested parties can contact the authors to receive a freely available and open copy of the data set.

References

[1] Wright, I. C., Neptune, R. R., van den Bogert, A. J., and Nigg, B. M., 2000, "The Influence of Foot Positioning on Ankle Sprains," J. Biomech., **33**(5), pp. 513–519.

[2] Budhabhatti, S. P., Erdemir, A., Petre, M., Sferra, J., Donley, B., and Cavanagh, P. R., 2007, "Finite Element Modeling of the First Ray of the Foot: A Tool for the Design of Interventions," ASME J. Biomech. Eng., **129**(5), pp. 750–756.

[3] Cheung, J. T., and Zhang, M., 2008, "Parametric Design of Pressure-Relieving Foot Orthosis Using Statistics-Based Finite Element Method," Med. Eng. Phys., **30**(3), pp. 269–277.

[4] Ker, R. F., Bennett, M. B., Bibby, S. R., Kester, R. C., and Alexander, R. M., 1987, "The Spring in the Arch of the Human Foot," Nature (London), **325**, pp. 147–149.

[5] Fauth, A. R., Hamel, J. A., and Sharkey, N. A., 2004, "In Vitro Measurements of First and Second Tarsometatarsal Joint Stiffness," J. Appl. Biomech., **20**(1), pp. 14–24.

[6] Aerts, P., Ker, R. F., De Clercq, D., Ilsley, D. W., and Alexander, R. M., 1995, "The Mechanical Properties of the Human Heel Pad: A Paradox Resolved," J. Biomech., **28**(11), pp. 1299–1308.

[7] Challis, J. H., Murdoch, C., and Winter, S. L., 2008, "Mechanical Properties of the Human Heel Pad: A Comparison Between Populations," J. Appl. Biomech., **24**(4), pp. 377–381.

[8] Miller-Young, J. E., Duncan, N. A., and Baroud, G., 2002, "Material Properties of the Human Calcaneal Fat Pad in Compression: Experiment and Theory," J. Biomech., **35**(12), pp. 1523–1531.

[9] Ledoux, W. R., and Blevins, J. J., 2007, "The Compressive Material Properties of the Plantar Soft Tissue," J. Biomech., **40**(13), pp. 2975–2981.

[10] Freed, A. D., and Diethelm, K., 2006, "Fractional Calculus in Biomechanics:

[3] https://simtk.org/home/multidomain.

A 3D Viscoelastic Model Using Regularized Fractional Derivative Kernels With Application to the Human Calcaneal Fat Pad," Biomech. Model. Mechanobiol., **5**(4), pp. 203–215.
[11] Huang, C. K., Kitaoka, H. B., An, K. N., and Chao, E. Y., 1993, "Biomechanical Evaluation of Longitudinal Arch Stability," Foot Ankle, **14**(6), pp. 353–7.
[12] De Clercq, D., Aerts, P., and Kunnen, M., 1994, "The Mechanical Characteristics of the Human Heel Pad During Foot Strike in Running: An In Vivo Cineradiographic Study," J. Biomech., **27**(10), pp. 1213–1222.
[13] Petre, M., Erdemir, A., and Cavanagh, P. R., 2008, "An MRI-Compatible Foot-Loading Device for Assessment of Internal Tissue Deformation," J. Biomech., **41**(2), pp. 470–474.
[14] Yavuz, M., Erdemir, A., Botek, G., Hirschman, G. B., Bardsley, L., and Davis, B. L., 2007, "Peak Plantar Pressure and Shear Locations: Relevance to Diabetic Patients," Diabetes Care, **30**(10), pp. 2643–2645.
[15] Zou, D., Mueller, M. J., and Lott, D. J., 2007, "Effect of Peak Pressure and Pressure Gradient on Subsurface Shear Stresses in the Neuropathic Foot," J. Biomech., **40**(4), pp. 883–890.
[16] Leardini, A., Benedetti, M. G., Berti, L., Bettinelli, D., Nativo, R., and Giannini, S., 2007, "Rear-Foot, Mid-Foot and Fore-Foot Motion During the Stance Phase of Gait," Gait and Posture, **25**(3), pp. 453–462.
[17] Erdemir, A., and Piazza, S. J., 2004, "Changes in Foot Loading Following Plantar Fasciotomy: A Computer Modeling Study," ASME J. Biomech. Eng., **126**(2), pp. 237–243.
[18] Camacho, D. L. A., Ledoux, W. R., Rohr, E. S., Sangeorzan, B. J., and Ching, R. P., 2002, "A Three-Dimensional, Anatomically Detailed Foot Model: A Foundation for a Finite Element Simulation and Means of Quantifying Foot-Bone Position," J. Rehabil. Res. Dev., **39**(3), pp. 401–410.
[19] Chen, W. P., Tang, F. T., and Ju, C. W., 2001, "Stress Distribution of the Foot During Mid-Stance to Push-Off in Barefoot Gait: A 3-D Finite Element Analysis," Clin. Biomech. (Bristol, Avon), **16**(7), pp. 614–620.
[20] Cheung, J. T., Zhang, M., Leung, A. K., and Fan, Y., 2005, "Three-Dimensional Finite Element Analysis of the Foot During Standing—A Material Sensitivity Study," J. Biomech., **38**(5), pp. 1045–1054.
[21] Gefen, A., Megido-Ravid, M., Itzchak, Y., and Arcan, M., 2000, "Biomechanical Analysis of the Three-Dimensional Foot Structure During Gait: A BasicT-tool for Clinical Applications," ASME J. Biomech. Eng., **122**(6), pp. 630–639.
[22] Janda, S., van der Helm, F. C. T., and de Blok, S. B., 2003, "Measuring Morphological Parameters of the Pelvic Floor for Finite Element Modelling Purposes," J. Biomech., **36**(6), pp. 749–757.
[23] Klein Breteler, M. D., Spoor, C. W., and Van der Helm, F. C., 1999, "Measuring Muscle and Joint Geometry Parameters of a Shoulder for Modeling Purposes," J. Biomech., **32**(11), pp. 1191–1197.
[24] Lachowitzer, M. R., Ranes, A., and Yamaguchi, G. T., 2007, "Musculotendon Parameters and Musculoskeletal Pathways Within the Human Foot," J. Appl. Biomech., **23**(1), pp. 20–41.
[25] Noble, L.D., Colbrunn, R.W., Lee, D.G., van den Bogert, A.J., and Davis, B.L., "Design and Validation of a General Purpose Robotic Testing System for Musculoskeletal Applications," ASME J. Biomech. Eng., accepted.
[26] Sirimamilla, P. A., 2008, "Elaborate experimentation for mechanical characterization of the human foot using inverse finite element analysis," MS thesis, Case Western Reserve University, Cleveland, OH.
[27] Cavanagh, P. R., 1999, "Plantar Soft Tissue Thickness During Ground Contact in Walking," J. Biomech., **32**(6), pp. 623–628.
[28] Fung, Y. C., 1993, *Biomechanics: Mechanical Properties of Living Tissues*, Springer, New York.
[29] Garner, B. A., and Pandy, M. G., 1999, "A Kinematic Model of the Upper Limb Based on the Visible Human Project (VHP) Image Dataset," Comput. Methods Biomech. Biomed. Eng., **2**(2), pp. 107–124.
[30] Noakes, K. F., Bissett, I. P., Pullan, A. J., and Cheng, L. K., 2008, "Anatomically Realistic Three-Dimensional Meshes of the Pelvic Floor & Anal Canal for Finite Element Analysis," Ann. Biomed. Eng., **36**(6), pp. 1060–1071.
[31] Ruan, J., El-Jawahri, R., Chai, L., Barbat, S., and Prasad, P., 2003, "Prediction and Analysis of Human Thoracic Impact Responses and Injuries in Cadaver Impacts Using a Full Human Body Finite Element Model," Stapp Car Crash J., **47**(Oct), pp. 299–321.
[32] Wu, L., 2007, "Nonlinear Finite Element Analysis for Musculoskeletal Biomechanics of Medial and Lateral Plantar Longitudinal Arch of Virtual Chinese Human After Plantar Ligamentous Structure Failures," Clin. Biomech. (Bristol, Avon), **22**(2), pp. 221–229.
[33] Söderkvist, I., and Wedin, P. A., 1993, "Determining the Movements of the Skeleton Using Well-Configured Markers," J. Biomech., **26**(12), pp. 1473–1477.
[34] Erdemir, A., Viveiros, M. L., Ulbrecht, J. S., and Cavanagh, P. R., 2006, "An Inverse Finite-Element Model of Heel-Pad Indentation," J. Biomech., **39**(7), pp. 1279–1286.
[35] Halloran, J. P., Erdemir, A., and van den Bogert, A. J., 2009, "Adaptive Surrogate Modeling for Efficient Coupling of Musculoskeletal Control and Tissue Deformation Models," ASME J. Biomech. Eng., **131**(1), p. 011014.

Post-print standardized by MSL Academic Endeavors, the imprint of the Michael Schwartz Library at Cleveland State University, 2014